Proceedings of the 20th International Conference on Soil Mechanics and Geotechnical Engineering– Rahman and Jaksa (Eds)
© 2022 Australian Geomechanics Society, Sydney, Australia, ISBN 978-0-9946261-4-1

Estimation of strength and stiffness of expandable foam grout using elastic and electromagnetic waves

Estimation de la résistance et de la rigidité du coulis mousse expansible à l'aide d'ondes élastiques et électromagnétiques

WooJin Han & Jong-Sub Lee & Junghee Park
School of Civil, Environmental and Architectural Engineering, Korea University, South Korea. kkl305@naver.com

Yong-Hoon Byun
School of Agricultural Civil & Bio-Industrial Engineering, Kyungpook National University, South Korea.

ABSTRACT: Expandable foam grout (EFG) is a highly flowable material developed for backfilling underground cavities. The objective of this study is to estimate the strength and stiffness of EFG based on the measurements of elastic and electromagnetic waves. Piezo disk elements and bender elements, which were installed in a mono cast nylon mold, were used to measure elastic waves. Four electrodes were installed at the edge of the mold to monitor electrical resistivity during curing time. The unconfined compressive strength of the EFG was also measured for the corresponding time. The results show that the elastic wave velocities rapidly increased for up to 3 days, and then gradually converged to a certain value. The electrical resistivity varied according to the curing stage of the EFG. The elastic wave velocities and electrical resistivity have strong relationships with the elastic moduli and strength of the EFG. Therefore, the elastic wave velocity and electrical resistivity can be used to estimate the strength and stiffness of the EFG during the curing time.

RÉSUMÉ: Coulis mousse expansible (expandable foam grout, EFG) est un matériau hautement fluide développé pour le remblayage de cavités souterraines. L'objectif de cette étude est d'estimer la résistance et la rigidité d'EFG à partir de la mesure des ondes élastiques et électromagnétiques. Les éléments de disque piézo et les éléments de cintrage, qui sont installés dans un moule en nylon monocast, sont utilisés pour mesurer les ondes élastiques. Quatre électrodes sont installées au bord du moule pour surveiller la résistivité électrique pendant le temps de durcissement. La résistance à la compression non confinée de l'EFG est également mesurée au moment correspondant. Les résultats montrent que les vitesses des ondes élastiques augmentent rapidement jusqu'à 3 jours puis convergent progressivement vers une certaine valeur. La résistivité électrique varie en fonction des étapes de durcissement de l'EFG. Les vitesses des ondes élastiques et la résistivité électrique ont de fortes relations avec les modules élastiques et la résistance de l'EFG. Par conséquent, la vitesse de l'onde élastique et la résistivité électrique peuvent être utilisées pour estimer la résistance et la rigidité de l'EFG pendant le temps de durcissement.

KEYWORDS: compressive strength; dynamic modulus; electrical resistivity; expansion; flowable fill

1 INTRODUCTION

In urban areas, deteriorated pipelines, underground excavations, and groundwater flow may result in leakage from pipelines or slurry walls. Soil erosion due to leakage may cause ground subsidence or underground cavities (Hong et al., 2018; Liu et al., 2019; Park and Hong, 2020). Underground cavities should be filled with a material or method to minimize traffic regulation.

Conventional methods to repair cavities use soils with compaction, however, soil compaction often generates vibration and noise. Moreover, improper compaction near buried pipelines or in narrow spaces can cause loose layers or even ground subsidence. Recently, the repair construction has used a high flowable and cementitious material such as controlled low-strength materials (CLSMs). CLSMs provide reduced construction time by self-compaction and low strength for re-excavation in pipeline repair (ACI 229R, 1999). However, construction with CLSM generally requires open-cut construction, whereas construction with expandable foam grout (EFG) only requires a space to inject the materials to minimize the regulated zone.

To proceed with the subsequent construction process, the curing status of constructed cementitious materials should be monitored. Therefore, non-destructive testing methods are required to evaluate the strength and stiffness of materials such as elastic and electromagnetic wave measurements. Most recently, Han et al. (2021) showed a series of relationships between engineering properties and wave characteristics of EFG.

In this study, the engineering properties and wave characteristics of EFG are reviewed, and new relationships are suggested to predict the compressive strength and static elastic modulus using elastic and electromagnetic waves.

2 EXPERIMENTAL SETUP

2.1 *Expandable Foam Grout*

EFG consists of water, ordinary Portland cement, and admixture. The admixture contains bentonite and aluminum powder. The aluminum powder induces volume expansion and pore development in cement paste generating hydrogen gas for the first 3 to 4 hours.

In this study, the water-cement ratio was determined as 100% considering the long-term strength which does not exceed 2.1 MPa. The admixture-cement ratio was determined as 4.0% considering the efficiency of volume expansion.

The EFG showed a high flow consistency of 540 mm in the flow test for CLSMs (ASTM D6103, 2017). Although the flow consistency exceeded 300 mm, the EFG did not produce bleed water in the expansion test which is similar to the bleeding test for grouting materials (ASTM C940, 2016). The expansion test was performed in a chamber at a constant temperature of 20 ^{o}C. The test results showed that the EFG volume expanded to the terminal expansion ratio of 44% compared to the initial volume of EFG at the slurry state.

2.2 *Unconfined Compressive Strength Test*

EFG specimens with a diameter of 50 mm and a height of 100 mm were prepared for unconfined compressive strength tests according to ASTM D4832 (2016). Mixed EFG filled in cylindrical molds whose height is longer than the specimens and was cured for a day. The expanded and overflowed EFG from the molds were leveled. The leveled specimens were demolded and trimmed to use in the compressive tests. The trimmed specimens were sealed to minimize moisture loss and cured for 3, 7, 14, and 28 days.

In this study, the apparatus for compressive tests equipped a loadcell with a capacity of 19.6 kN was used with a loading rate of 1 mm/min. To determine the compressive strength, at least three specimens were tested considering the repeatability, and the results were averaged except for outliers.

2.3 *Elastic Wave Measurement System*

Elastic wave measurement is a non-destructive method to evaluate the stiffness of cementitious materials. In this study, compressional and shear waves generated by embedded transducers in an MC nylon mold were measured for 28 days as shown in Figure 1. Piezoelectric disk elements (PDEs) and bender elements (BEs) generated and received the compressional and shear waves propagating through an EFG specimen cured in the mold, respectively. The input signal was a square wave with a frequency of 20 Hz and an amplitude of 10V. Square waves provide a clear response because they include all frequency components when the resonant frequency is unknown (Lee and Santamarina, 2005).

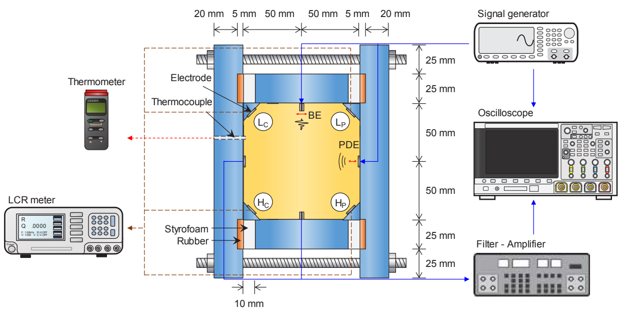

Figure 1. Measurement system for elastic wave and electrical resistivity.

2.4 *Electrical Resistivity Measurement System*

Electrical resistivity was correlated with the strength of cementitious materials to predict the strength in previous studies (Polder, 2001; Ferreira and Jalali, 2010). Because electrical resistivity is related to electrical conductivity, the resistivity can capture the chemical changes caused by cement hydration in cementitious materials. The curing process of the EFG also includes hydrogen gas generation by the aluminum reaction.

Figure 1 shows the measurement of the electrical resistance to evaluate the electrical resistivity of the EFG over the curing time. To estimate the electrical resistance, four electrodes were installed with a square array configuration in the columns at the edge of the mold (Kang and Lee, 2015). The operating frequency was determined as 1 kHz from frequency sweeping tests. In addition, the temperature in the EFG specimen was monitored using a k-type thermocouple to compensate for the temperature effects on the measured resistance.

Considering temperature compensation, the relationship between the electrical resistivity (r_{es}) and electrical resistance at a certain temperature (R_T) was established as shown in Eq. 1.

$$r_{es} = 0.666R_T[1 - 0.027(20 - T)] \quad (1)$$

3 EXPERIMENTAL RESULTS

3.1 *Unconfined Compressive Strength*

From the compressive strength tests, stress-strain curves were obtained for specimens cured for 3, 7, 14, and 28 days. The stress-strain curves provide the compressive strength and static elastic modulus. The peak stress in a stress-strain curve is the compressive strength and the static elastic modulus is determined from Eq. 2.

$$E_{50} = (0.5f_c/\varepsilon_{50}) \times 100 \quad (2)$$

where E_{50} and f_c are the secant elastic modulus and compressive strength, respectively, and ε_{50} denotes the strain corresponding to half of its compressive strength.

Figure 2 shows the unconfined compressive strength and static elastic modulus estimated from the stress-strain curves for each curing time. The overall trends for both compressive strength and elastic modulus showed the logarithmic functions of the curing time.

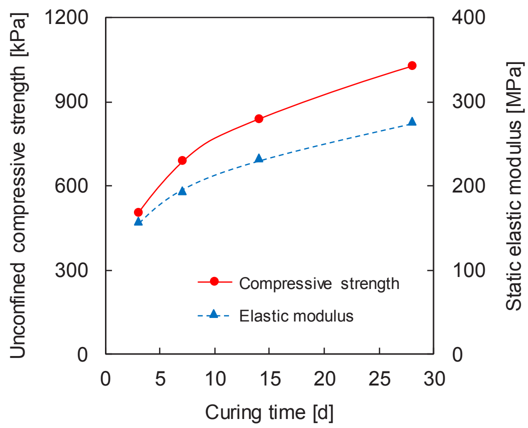

Figure 2. Variations in unconfined compressive strength and static elastic modulus over the curing time.

3.2 *Elastic Wave Velocities*

Elastic wave velocities were estimated using the first arrival time obtained from the compressional and shear wave signals, and plotted in Figure 3. Both elastic wave velocities increased with curing time, but their slopes gradually decreased with the curing time. The compressional wave velocity (V_P) of 656 m/s at 3 days increased to 1311 m/s at 28 days. The shear wave velocity (V_S) of 367 m/s at 3 days increased to 673 m/s at 28 days.

From the elastic wave velocities, the dynamic elastic modulus can be estimated as shown in Eqs. 3 and 4.

$$M_d = \rho V_P^2 \quad (3)$$

$$G_d = \rho V_S^2 \quad (4)$$

where M_d and G_d denote the dynamic constrained and shear modulus, respectively, and ρ is the density of the EFG specimen which remained constant after curing for 3 days at 0.85 g/cm^3.

3.3 *Electrical Resistivity*

Figure 4 showed the electrical resistivity and temperature for the curing time. The electrical resistivity increased with the increase in curing time, but temperature was almost constant at room temperature of 20 °C.

The increasing electrical resistivity indicates that the water content in the EFG specimen decreases owing to cement hydration and evaporation and the water content loss reduced the ionic mobility.

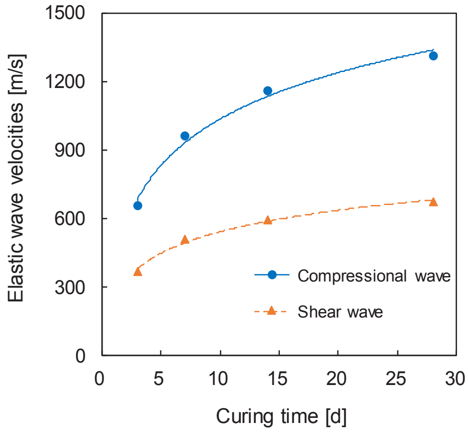

Figure 3. Compressional and shear wave velocities with curing time.

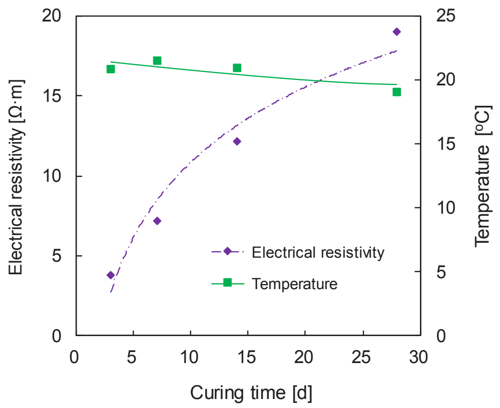

Figure 4. Variations in electrical resistivity and temperature over curing time.

4 DISCUSSION

4.1 *Dynamic Elastic Modulus*

Yao et al. (2019) organized previous studies about relationships between the unconfined compressive strength and dynamic elastic modulus estimated from Eqs. 3 and 4. According to Yao et al. (2019), cemented soils showed the linear relationships between the strength and dynamic moduli. In this study, the relationships between the dynamic moduli and compressive strength were established by the following linear functions:

$$f_c = 0.47M_d + 325 \qquad (R^2 = 0.994) \qquad (5)$$

$$f_c = 1.93G_d + 275 \qquad (R^2 = 0.996) \qquad (6)$$

In addition, the static elastic modulus can be expressed as function of the dynamic elastic moduli. Lydon and Balendran (1986) proposed a linear relationship between the static and dynamic moduli for concrete. The relationships for the EFG can also be expressed by the following linear functions:

$$E_S = 0.11M_d + 325 \qquad (R^2 = 0.990) \qquad (7)$$

$$E_S = 0.45G_d + 102 \qquad (R^2 = 0.990) \qquad (8)$$

Figure 5. Relationship between unconfined compressive strength and

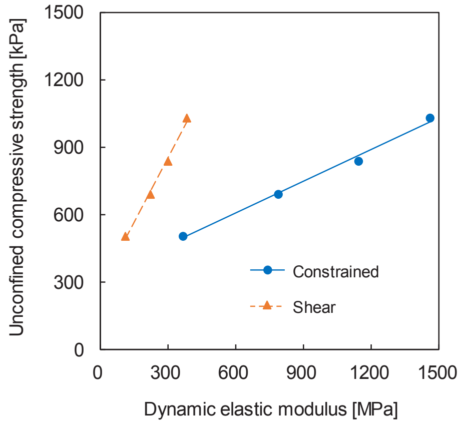

dynamic moduli.

4.2 *Electrical Resistivity*

The cementitious materials develop their strength and stiffness by chemical reactions such as cement hydration. Therefore, the variations in electrical resistivity can represent the variations in the strength and stiffness of cementitious materials.

Previous studies described the relationships with electrical resistivity as linear functions (Ferreira and Jalali, 2010; Wei et al., 2012). Figure 6 shows the estimated relationships between the compressive strength and static elastic modulus Their equations were expressed by linear functions as follows:

$$f_c = 33.3r_{es} + 416 \qquad (R^2 = 0.978) \qquad (9)$$

$$E_S = 7.76r_{es} + 134 \qquad (R^2 = 0.987) \qquad (10)$$

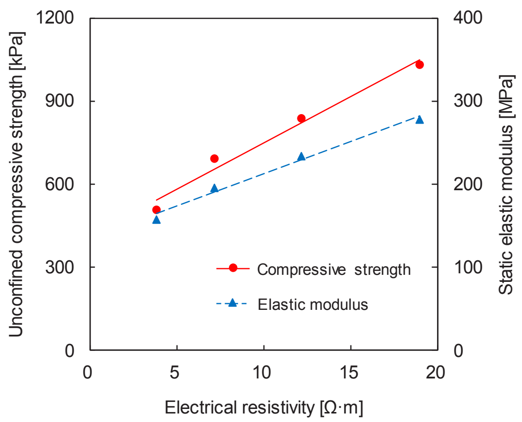

Figure 6. Variation in unconfined compressive strength and static elastic modulus with respect to electrical resistivity.

5 CONCLUSIONS

This study proposed relationships to predict the compressive strength and static elastic modulus of expandable foam grout (EFG). Elastic wave velocities and electrical resistivities were monitored during curing time using elastic and electromagnetic waves.

The compressive strength and static elastic modulus increased along logarithmic functions of the curing time. Moreover, the compressional and shear wave velocities increased with the increase in curing time. Electrical resistivity also increased as curing time increased. The compressive strength and static elastic modulus can be expressed as functions of constrained and shear moduli estimated from elastic wave velocities. These relationships are presented as linear equations with a high goodness of fit. The compressive strength and static elastic modulus can also be expressed as linear functions of electrical resistivity.

Therefore, the elastic wave velocity and electrical resistivity can be used to estimate the strength and stiffness of the EFG during the curing time.

6 ACKNOWLEDGEMENTS

This research was supported by Basic Science Research Program through the National Research Foundation of Korea (NRF) funded by the Ministry of Science, ICT & Future Planning (NRF-2020R1A2B5B03001470).

7 REFERENCES

American Concrete Institute Committee 229 1999. ACI 229R-99: Report on controlled low-strength materials. *American Concrete Institute (ACI)* Farmington Hills, MI, USA.

ASTM C940 2016. Standard Test Method for Expansion and Bleeding of Freshly Mixed Grouts for Preplaced-Aggregate Concrete in the Laboratory. *ASTM International* West Conshohocken, PA.

ASTM D4832 2016. Standard test method for preparation and testing of controlled low strength material (CLSM) test cylinders. *ASTM International* West Conshohocken, PA.

ASTM D6103/6103M 2017. Standard test method for flow consistency of controlled low strength material (CLSM). *ASTM International*, West Conshohocken, PA.

Ferreira R.M. and Jalali S. 2010. NDT measurements for the prediction of 28-day compressive strength. *NDT E Int.* 43(2), 55-61.

Han W.J., Lee J.S., and Byun Y.H. 2021 Volume, strength, and stiffness characteristics of expandable foam grout. *Constr. Build. Mater.* 274, 122013.

Hong W.T., Kang S., Lee S.J., and Lee J.S. 2018. Analyses of GPR signals for characterization of ground conditions in urban areas. *J. Appl. Geophys.* 152, 65-76.

Liu X.X., Shen S.L., Zhou A., and Xu Y.S. 2019. Evaluation of foam conditioning effect on groundwater inflow at tunnel cutting face. *Int. J. Numer. Anal. Methods in Geomech.* 43(2), 463-481.

Lydon F.D. and Balendran R.V. 1986. Some observations on elastic properties of plain concrete. *Cement and Concrete Res*. 16(3), 314-324.

Park J. and Hong G. 2020. Strength Characteristics of Controlled Low-Strength Materials with Waste Paper Sludge Ash (WPSA) for Prevention of Sewage Pipe Damage. *Materials* 13(19), 4238.

Polder R.B. 2001. Test methods for on site measurement of resistivity of concrete—a RILEM TC-154 technical recommendation. *Constr. and Build. Mater.* 15(2-3), 125-131.

Wei X., Xiao L. and Li Z. 2012. Prediction of standard compressive strength of cement by the electrical resistivity measurement. *Constr. Build. Mater.* 31, 341-346.

Yao K., Xiao H., Chen D.H. and Liu Y. 2019. A direct assessment for the stiffness development of artificially cemented clay. *Géotechnique* 69(8), 741-747.